1985

Comparison of proton transfers in (S2H5)+ and (O2H5)+

L. Bigham

Steve Scheiner
Utah State University

Recommended Citation
Comparison of proton transfers in (S[sub 2]H[sub 5])[sup +] and (O[sub 2]H[sub 5])[sup +] Steve Scheiner and Larry D. Bigham, J. Chem. Phys. 82, 3316 (1985), DOI:10.1063/1.448230

Comparison of proton transfers in $(S_2H_5)^+$ and $(O_2H_5)^+$

Steve Scheiner[a),b)] and Larry D. Bigham
Department of Chemistry and Biochemistry, Southern Illinois University, Carbondale, Illinois 62901

(Received 26 July 1984; accepted 21 December 1984)

The energetics and electronic rearrangements associated with proton transfer between S atoms in $(H_2S–H–SH_2)^+$ are calculated using *ab initio* molecular orbital methods and compared with similar data in the first-row analog $(H_2O–H–OH_2)^+$. The full potential energy surface of $(S_2H_5)^+$, calculated as a function of the H-bond length as well as the position of the proton, contains two equivalent minima separated by a small energy barrier, whereas the surface of $(O_2H_5)^+$ contains a single minimum corresponding to a symmetric position for the central proton. In both cases the energy barrier to transfer increases as the H bond is lengthened. This rise is noticeably less steep in the case of $(S_2H_5)^+$, a fact attributed to the greater ease with which a proton may be pulled a given distance from each SH_2 subunit in the absence of the other. Enlargements of the proton transfer barriers also result from angular distortions of each H bond; these increases are qualitatively quite similar in the two systems. There is a great deal of resemblance also in the electronic redistribution patterns accompanying proton transfer in the two systems. However, the greater polarizability of SH_2 as compared to OH_2 leads to greater overall charge transfer between the subunits in $(H_2S–H–SH_2)^+$ and to larger extent of spatial regions of density change.

I. INTRODUCTION

In tandem with experimental studies,[1–8] *ab initio* theoretical investigations of proton transfer reactions[9–24] have contributed a great deal to our knowledge of this process. Most of these theoretical treatments have dealt with systems involving oxygen and nitrogen atoms due to their common occurrence in H bonds. However, atoms of the second row of the Periodic Table are also capable of forming H bonds and information regarding proton transfers in such bonds would thus be quite useful. Moreover, comparison between first- and second-row analogs may be expected to be interesting from a fundamental perspective. Calculations were carried out recently in this laboratory[25] treating proton transfers between the oxygen atoms of $(H_2O–H–OH_2)^+$. Energetics were reported for both stretches and bends of the H bond and electronic structural features were examined as well. The present communication reports the results of similar calculations involving the second-row analog $(H_2S–H–SH_2)^+$ and compares these data with the previous results for $(H_2O–H–OH_2)^+$. This paper thus represents the first *ab initio* study of proton transfer within the proton-bound SH_2 dimer.

The first section reports the results of geometry optimizations of the $(H_2S–H–SH_2)^+$ complex and the strength of the H bond. Proton transfers are considered in Sec. II B, including an evaluation of the accuracy of the theoretical approach. In Sec. II C, the redistributions of electronic density which accompany the shift of the proton along the H bond are described and contrasted with analogous properties of the oxygen-containing system. Section II D contains an analysis of the effects of angular distortions of the H bond upon the energetics of proton transfer.

II. METHODS AND RESULTS

To ensure proper comparison with the previous SCF calculations of $(O_2H_5)^+$ where the 4-31G basis set[26] was employed, the present study of $(S_2H_5)^+$ made use of the same computational procedure. This method has been used successfully in the past to study the H bond[27] of $(H_2S–H–SH_2)^+$ as well as proton transfers in other systems.[25,28,29] All calculations were carried out with the GAUSSIAN 70 and 80 programs.[30,31] As described below, the sensitivity of the results to basis set was studied via comparison with larger sets including polarization functions and the effects of electron correlation were investigated by second and third-order Møller–Plesset perturbation theory.

A. Optimized geometry and binding energy of $(S_2H_5)^+$

The structure of $(H_2S–H–SH_2)^+$ was fully optimized subject to the following constraint. The central proton was assumed to lie along the S--S axis as shown in Fig. 1, in conformity with the calculations of this system by Desmeules and Allen.[27] Our own calculations of similar systems[28,32] have indicated that deviations from linearity are rather small. The symmetry adopted by the complex is C_s, as illustrated in Fig. 1. The parameters of the fully optimized complex are contained in the first column of Table I where it may be seen that the R(SS) H-bond length is 3.482 Å. The central proton lies 1.462 Å from the left sulfur atom S^a, much closer than the 2.020 Å from the other S atom. Thus, the equilibrium geometry contains an asymmetric H bond, in contrast to the

a) To whom correspondence should be addressed.
b) Recipient of NIH Research Career Development Award (1982–87).

 0021-9606/85/073316-06$02.10

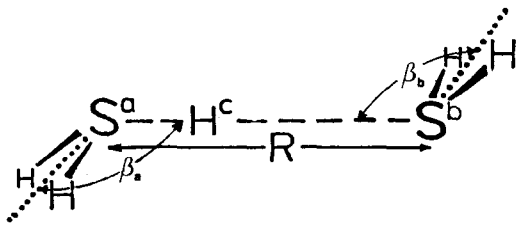

FIG. 1. Geometry of $(S_2H_5)^+$ system belonging to C_s point group. β_a and β_b refer to angles between the S--S axis and the bisectors of the two SH_2 subunits.

symmetric H bond in the $(O_2H_5)^+$ analog where the most stable position of the central proton is precisely midway between the two O atoms.

The difference in energy between the $(S_2H_5)^+$ complex and the sum of the optimized SH_2 and $(SH_3)^+$ species is listed as E^D in the last row of Table I and corresponds to the dissociation energy of the complex. The computed value of 16.8 kcal/mol is reasonably close to recent experimental estimates[33] in the range 12.8–15.4 kcal/mol. This H-bond energy is considerably smaller than the corresponding experimental value[33] of 33 kcal/mol for $(H_2O–H–OH_2)^+$, consistent with the commonly accepted notion that H bonds between second-row atoms are weaker than their first-row counterparts. A second measure of the relative H-bond strengths comes from a comparison of the computed X–H--X H-bond lengths with the sum of the heavy atom van der Waals radii.[34] The latter quantity is 3.70 Å for a S–H--S bond and 2.80 for O–H--O. The actual computed H-bond length[25] for $(H_2O–H–OH_2)^+$ is 2.36 Å, representing a contraction of 0.44 Å when compared to the sum of oxygen van der Waals radii. The corresponding reduction in $(H_2S–H–SH_2)^+$ is only 0.22 Å, indicating again that the H bond is considerably weaker in complexes involving second-row atoms.

Most of the features of the internal geometries of the two SH_2 units in the complex are fairly similar to one another with the exception of the angles β_a and β_b which represent the orientations of the two subunits with respect to the S--S axis. The larger value of β_b is due to an electrostatic interaction between the two subunits. The dipole moment of the SH_2 molecule on the right is aligned along the HSH bisector, denoted by the dotted line in Fig. 1. The negative end of this dipole can most effectively point toward the positive charge of the left-hand $(SH_3)^+$ subunit for large values of β_b. Similar arguments have been used to explain intermolecular orientations in a number of related systems.[29]

TABLE I. Optimized geometries and energies of $(S_2H_5)^+$.

	$(H_2SH--SH_2)^+$	$(H_2S--H--SH_2)^+$
R(SS), Å	3.482	3.37
$r(S^aH^c)$, Å	1.462	1.685
$r(S^aH)$, Å	1.352	1.351
$r(S^bH)$, Å	1.351	1.351
$\theta(HS^aH)$	99.2°	98.5°
$\theta(HS^bH)$	97.8°	98.5°
β_a	106.8°	108.6°
β_b	114.1°	108.6°
E^{SCF}, a.u.	−796.690 59	−796.689 64
E^D, kcal/mol	16.8 (12.8–15.4)[a]	

[a] Experimental value from Ref. 33.

B. Proton transfers

The potential energy curve for proton transfer between the two S atoms was computed for each of a set of H-bond lengths R(SS) as follows. The system was frozen in the geometry of the optimized complex described in Table I and a value of R(SS) chosen. The central proton H^c was then shifted along the internuclear S--S axis, generating a transfer potential. The general shape of each curve contains two equivalent minima with an energy barrier separating them. The height of this energy barrier is denoted $E^\dagger$ and is illustrated as a function of the H-bond length R by the right-hand curve in Fig. 2. It is clear that the energy barrier to proton transfer rises quickly as the H bond is elongated. For H-bond lengths of less than approximately 3.28 Å, the barrier vanishes and the potential contains a single minimum corresponding to the S--H--S configuration in which the proton is midway between the two S atoms.

The corresponding proton transfer barriers in the oxygen analog[25] $(O_2H_5)^+$ are represented by the left-hand curve in Fig. 2 where generally similar behavior may be noted. One difference between the two systems is brought out by a comparison of the equilibrium H-bond length with that for which the barrier vanishes and the potential collapses into a single minimum. The proton transfer barrier for $(S_2H_5)^+$ reaches zero at 3.28 Å, 0.2 Å less than the equilibrium R(SS) distance of 3.48 Å, at which point the barrier is equal to 1.6 kcal/mol. In contrast, the barrier is zero and the potential contains a single minimum for the optimized R(OO) distance of 2.36 Å in $(O_2H_5)^+$.

A second distinction between the two curves in Fig. 2 is related to their slopes. The curve representing the rise of transfer barrier between sulfur atoms is clearly less steep than is the case for interoxygen transfer. This difference may be traced back to the shapes of the potentials associated with the dissociation of a proton from the individual XH_2 molecules: $(H_2X–H)^+ \rightarrow H_2X + H^+$. The proton dissociation curve calculated for SH_2 using the 4-31G basis set was found to be substantially less steep than that for OH_2. As described in a previous

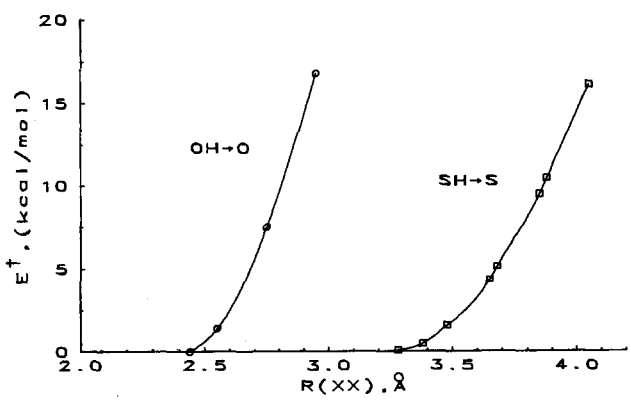

FIG. 2. Energy barriers to proton transfer as a function of the H-bond length R(XX). OH → O refers to the $(O_2H_5)^+$ system and SH → S to $(S_2H_5)^+$.

work,[29] a good first approximation to the proton transfer barrier may be obtained by appropriate superposition of the proton dissociation curves. Similar addition of the potentials here leads to the conclusion that the more gradual increase in proton transfer barrier height with H-bond length in $(H_2S–H–SH_2)^+$ is due to the smaller energy increments needed to pull a proton a given distance from its equilibrium position in $(H_2S–H)^+$.

The transfer barriers reported in Fig. 2 were computed using the rigid molecule approximation wherein all nuclei are held fixed in position as the proton is translated along the H-bond axis. Perhaps a more valid means of calculating these potentials would involve geometry optimizations at each stage of the transfer. Although previous calculations have demonstrated quite good agreement between the energetics obtained by the two approaches in a number of similar systems,[25,28,29] the validity of the rigid molecule approximation was checked for $(S_2H_5)^+$. It was found that transfer barriers calculated including geometry optimizations were within 0.4 kcal/mol of those contained in Fig. 2 for all values of R. In addition, the optimizations led to only very small changes in the intramolecular geometries; bond lengths were constant to within 0.002 Å and bond angles to 1°.

As a last point, we consider a model of proton transfer in which *all* geometrical parameters, including the H-bond length, are allowed to change as the proton is shifted across the bond. Whereas the previous transfers with fixed R(XX) model proton shifts within the rigid framework of a macromolecule, optimization of this distance during the transfer process corresponds to the more flexible situation of the isolated $(S_2H_5)^+$ system in the gas phase. The energy barrier for this "flexible" transfer is equal to the difference in energy between the fully optimized $(H_2SH\text{--}SH_2)^+$ complex described above and listed in the first column of Table I and that of $(H_2S\text{--}H\text{--}SH_2)^+$ in which the central proton is restricted to lie equally distant from the two S nuclei (C_{2h} symmetry). The geometry of the latter complex is contained in the last column of Table I from which it may be seen that the R(SS) H-bond length in this transition state to proton transfer is 3.37 Å, 0.11 Å shorter than in the fully optimized $(H_2SH\text{--}SH_2)^+$ configuration. This shortening in the transition state is characteristic of these proton transfer processes and has been noted previously in a number of cases.[32,35,36] The barrier for this proton transfer between the two equivalent minima in the potential energy surface is found to be equal to 0.6 kcal/mol, in contrast to $(O_2H_5)^+$ for which the surface contains a single minimum corresponding to symmetric $(H_2O\text{--}H\text{--}OH_2)^+$.

1. Accuracy of results

Since there is no *a priori* reason to expect SCF-level calculations using the 4-31G basis set to be of high accuracy, it was necessary to gauge the results against data computed at higher levels of theory. The basis set was enlarged in two steps. First, a single set of 6 d functions (exponent = 0.39)[37] was added to each S center; this basis set is denoted as 4-31G*. The largest set used[38] involved a [6s, 4p] contraction of 12s and 8p Gaussian primitives on each S; a set of d functions (ζ = 0.6) was added as well. A triple-ζ contraction of five s primitives was used for the central hydrogen and was augmented by a set of p functions with exponent 1.0. The remaining hydrogens were described by a double-ζ contraction of (4s) primitives and a scale factor of 1.2. The latter basis set is referred to here as [641/31/2]. The effects of electron correlation were included via second and third-order Møller–Plesset perturbation theory[39] (MP2 and MP3).

Potentials for proton transfer in $(S_2H_5)^+$ for the equilibrium R(SS) distance of 3.482 Å were computed for each of several levels of theory. The transfer barriers, evaluated as the difference in energy between the minimum and maximum of each potential,[40] are reported in Table II. It is clear from examination of any column that each successive enlargement of the basis set leads to an increase in the transfer barrier. The opposite trend of a barrier decrease results from incorporation of electron correlation. Specifically, the MP2 barriers are considerably smaller than the SCF values, while carrying the perturbation expansion to third order produces a small increase over the MP2 barriers. These trends are consistent with previous findings in similar systems.[32,35,36] At the highest level of theory considered here, the MP3/[641/31/2] barrier is somewhat higher than the HF/4-31G value, leading to the conclusion that the barriers computed via the latter procedure are probably uniformly smaller than the true values. Therefore, we expect that use of the MP3/[641/31/2] procedure throughout would yield a potential energy surface with a more pronounced barrier separating the two minima; we estimate an adiabatic transfer barrier of 1 to 2 kcal/mol.

C. Electronic rearrangements

Examination of electronic structure provides a key means of analyzing fundamental features of various chemical processes. In the case of the proton transfer reaction, a good deal of information has accrued through scrutiny of the redistributions of electron density that accompany the shift of the proton.[28,29,41] We focus our attention here upon a comparison between the isovalent $(S_2H_5)^+$ and $(O_2H_5)^+$ systems to determine the different properties of first and second-row atoms when participating in the proton transfer process.

The changes in Mulliken populations resulting from half-transfer of the central proton in the two systems are reported in Table III. In accord with previous nomenclature,[28] the a superscript indicates the proton-donating subunit while the acceptor is denoted by b. In order to ensure consistency of data for purposes of comparison, a number of unifying factors were included. First, since previous calculations[25,28] treated a planar $(O_2H_5)^+$ system, the sulfur-containing analog was similarly flattened by

TABLE II. Proton transfer barriers computed for $(S_2H_5)^+$ for R = 3.482 Å. All entries in kcal/mol.

Basis set	SCF	MP2	MP3
4-31G	1.6	0.5	0.6
4-31G*	4.4	1.7	2.0
[641/31/2]	5.7	2.8	3.2

TABLE III. Changes in Mulliken populations (in me) caused by half-transfer of the central proton. Positive entries correspond to density increase. X represents either S or O atom; orbitals shown are valence shell (e.g., 2*s* for O and 3*s* for S). Central proton moves 0.279 Å in all cases.

	$(O_2H_5)^+$ R = 2.75 Å planar	$(S_2H_5)^+$ R = 3.482 Å planar	$(S_2H_5)^+$ R = 3.482 Å pyramidal
Groups			
$(XH_2)^a$	91	152	161
$(XH_2)^b$	−77	−149	−171
Atoms			
H^c	−14	−3	10
X^a	30	68	99
H^a	30	42	31
X^b	−11	−57	−103
H^b	−33	−46	−34
Orbitals (X^a)			
s	15	51	6
p_z	59	53	156
p_x	−45	−36	−34
p_y	0	0	−28
Orbitals (X^b)			
s	−12	−49	−6
p_z	−44	−45	−158
p_x	45	37	35
p_y	0	0	26

[a] Proton donor.
[b] Proton acceptor.
[c] Central proton.

setting both β_a and β_b (see Fig. 1) equal to 180°. Secondly, at the equilibrium S--S distance of 3.482 Å, the central proton translates a total of 0.279 Å from its most stable position to reach the midpoint of the bond, whereas a somewhat longer distance is involved in the transfer in $(O_2H_5)^+$. Since the density redistributions are sensitive to the distance moved by the proton,[28] the latter distance was shortened to 0.279 Å in $(O_2H_5)^+$. The data for planar $(O_2H_5)^+$ and $(S_2H_5)^+$ are contained in the first two columns of Table III, respectively.

A number of the trends seen in Table III are typical of proton transfer processes that have been examined in the past.[28] The first two rows indicate an overall shift of density from the proton-accepting subunit $(XH_2)^b$ to the proton donor $(XH_2)^a$. The charge extracted from the former subunit originates on the hydrogen atoms H^b as well as the X^b (O or S) atom; similarly, charge accumulation is observed on H^a as well as X^a. With regard to the atomic orbitals of the O and S atoms, the p_x orbital, perpendicular to the H-bond axis and lying in the molecular plane, follows a trend opposite in sign to the *s* and p_z orbitals. This observation has been attributed to polarization of the internal X–H bonds of each subunit which allow the hydrogen atoms to share in the overall density change of the entire subunit.[41]

Similar patterns emerge from another perspective via the contour maps of the charge redistribution that takes place in concert with the half transfer of the proton.[28] Such maps are provided in Fig. 3 where the central arrow denotes the movement of the proton; solid contours represent increases in electron density and broken contours decreases. The overall loss of density by the proton-accepting group is confirmed by the many broken contours surrounding the right-hand XH_2 subunit. The solid contours above and below the X^b atom are pictorial verification of the charge accumulation noted above for the p_x orbitals of this atom; changes of the opposite sign occur for the left-hand subunit.

Since the major thrust of the present communication is a comparison of the proton transfer properties of oxygen and sulfur, we turn now to the differences between the electronic rearrangement patterns taking place in $(O_2H_5)^+$ and $(S_2H_5)^+$. From the first two rows of Table

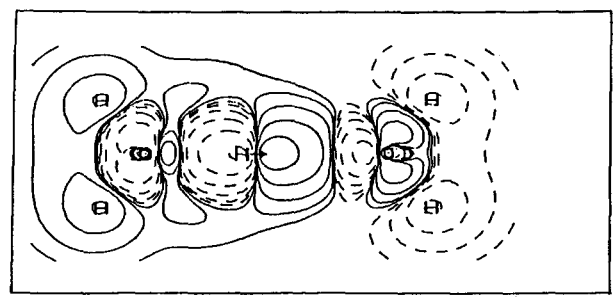

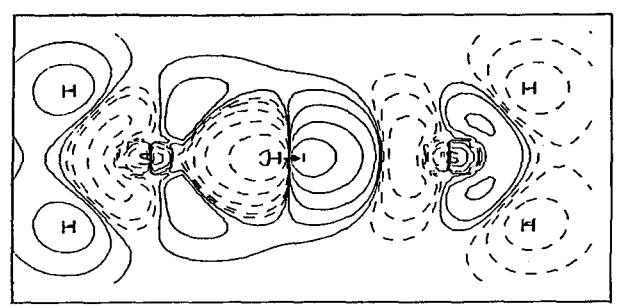

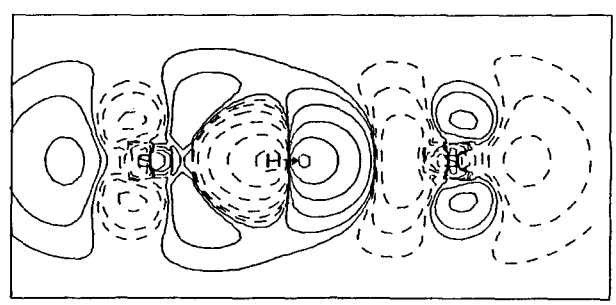

FIG. 3. Contour maps showing electron density rearrangements upon half-proton transfer in (a) $(O_2H_5)^+$, (b) planar $(S_2H_5)^+$, and (c) pyramidal $(S_2H_5)^+$. The arrow indicates the motion of the central proton (0.279 Å in all cases). Solid contours denote density increase and losses are shown by broken contours; the scale for the contours is logarithmic, ranging from $10^{-7/2}$ to $10^{-3/2}$ *e*/a.u.^{3}. The plane illustrated is *xz* which contains all atoms in a and b. The bending of the SH_2 subunits in c takes the noncentral hydrogens out of the *xz* plane.

III, we see that the shifts of density between the two subunits are of substantially greater magnitude in the latter system, probably due in large part to the greater polarizability of SH_2 than of OH_2. Most of the increased density change is directly attributable to the S atom rather than to the hydrogens. For example, the decrease in the S^b atom (57 *me*) is several times greater than in O^b (11 *me*) while the corresponding decrease in H^b rises only slightly from 33 to 46 *me*. With regard to the orbitals, the principal difference between O and S is the greater involvement of the *s* orbitals in the latter case; e.g., the increase in the *s* orbital of X^a rises from 15 to 51 *me* on going from O to S.

The clearest pictorial indication of the greater polarizability of the SH_2 subunit is the larger extent of the contours in Fig. 3(b). In particular, the broken contours to the left of S^b cover a much wider expanse than the corresponding region of charge loss to the left of O^b in Fig. 3(a). This difference helps account also for the atomic population data described above. It may be noted that the similar spatial characteristics of the contours in the vicinity of the noncentral hydrogens in Figs. 3(a) and 3(b) are consistent with the small differences between H population changes of the two systems in Table III.

It was pointed out above that the angles β_a and β_b were set equal to 180° in computing the density changes in Fig. 3(b) for the sake of comparison with the planar oxygen atoms in Fig. 3(a) although the equilibrium structure of $(S_2H_5)^+$ contains pyramidal arrangements about the S atoms. In order to determine the effects of this geometry change from a planar system on the electronic rearrangements, analogous data were calculated for the optimized pyramidal structure and the results reported in Fig. 3(c) and the last column of Table III. [Note the absence of the noncentral H atoms from the *xz* plane of Fig. 3(c).] Comparison of the second and third columns of Table III indicates that pyramidalization of the sulfur atoms leads to a small increase in the total charge transferred between (SH_2) subunits. This increase is drawn exclusively from the S atoms as the density changes associated with the noncentral hydrogens are reduced in magnitude. The enhanced charge loss associated with the S^b atom (nearly double) is indicated by the enlargements of the region enclosed by the dashed contours to its immediate left. Moreover, a new region of charge loss appears on the right side of this atom, in a position consistent with a good deal of density depletion from the p_z orbital which lies along the H-bond axis. Indeed, this charge loss is corroborated by the entry of −158 *me* for this orbital in the last column of Table III. While the p_x orbital is little affected by the pyramidalization, the bending of the hydrogen atoms out of the *xz* plane allows the p_y orbital to participate in the polarizations of the X–H bonds; hence, the increase in the p_y population of X^b. Very similar trends (of opposite sign) are noted in the proton-donating $(SH_2)^a$ subunit.

In summary, many of the patterns of charge redistribution noted previously for oxygen-containing systems occur as well in the case of sulfur. The greater polarizability of the latter atom leads to overall greater magnitude of density shifts which occur over larger spatial areas. Bending of the two SH_2 subunits to a pyramidal rather than planar configuration about each sulfur appreciably magnifies the above trends and localizes more of the density shifts onto the S atoms.

D. Angular deformations

The previous sections have dealt with H bonds in which the two subunits have been free to adopt their most energetically favorable orientations with respect to one another. However, when these bonds occur within the confines of a large molecule, e.g., when the O and S atoms are covalently attached to the backbone of a macromolecule, each bond will generally be somewhat distorted to satisfy the requirements of overall lowest energy of the entire molecule. In order to simulate the effects of such distortions upon the proton transfer process, the geometries of the H-bonded systems have been systematically modified as follows. First, in order to ensure a valid comparison between the sulfur and oxygen-containing systems, the fully planar configurations of both $(S_2H_5)^+$ and $(O_2H_5)^+$ were used as a starting point. The left-hand XH_2 subunit was rotated by an amount α_a with respect to the X--X axis, as shown in Fig. 4; rotation of the right-hand XH_2 subunit is described by the angle α_b. For each configuration, represented by the H-bond length R and the two rotation angles α_a and α_b, the proton transfer potential was generated by shifting the central proton along its minimum energy path between the two subunits. (This path did not generally lie along the X--X internuclear axis, as indicated by the position of the central proton in Fig. 4.) The positions of all other nuclei were held fixed as the proton was transferred.

Three different modes of angular deformation were considered. In the first mode, the left-hand molecule is unaffected while the right-hand subunit is rotated by an amount α_b. The effects of this type of distortion are represented by the solid curves in Fig. 5. The dashed curves correspond to a conrotatory motion wherein the two subunits are rotated by equal amounts and in the same direction. The disrotatory mode in which the two molecules are rotated in opposite directions are associated with the dotted curves in Fig. 5.

The effects of these angular distortions in $(O_2H_5)^+$ have been previously elucidated[25] and are presented on the left half of Fig. 5. Each mode leads to progressively higher barriers as the amount of the distortion is increased. For all three H-bond distances between 2.55 and 2.95 Å, the greatest barrier enlargement is associated with the disrotatory deformation and the smallest with rotation of only one subunit. The analogous data are presented on

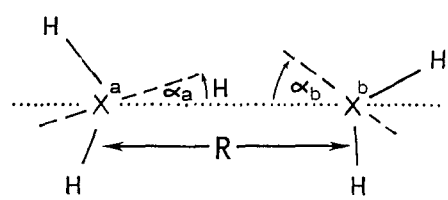

FIG. 4. Definition of parameters α_a and α_b used to specify angular distortions of the two SH_2 subunits. Dashed lines indicate bisectors of the HSH angles.

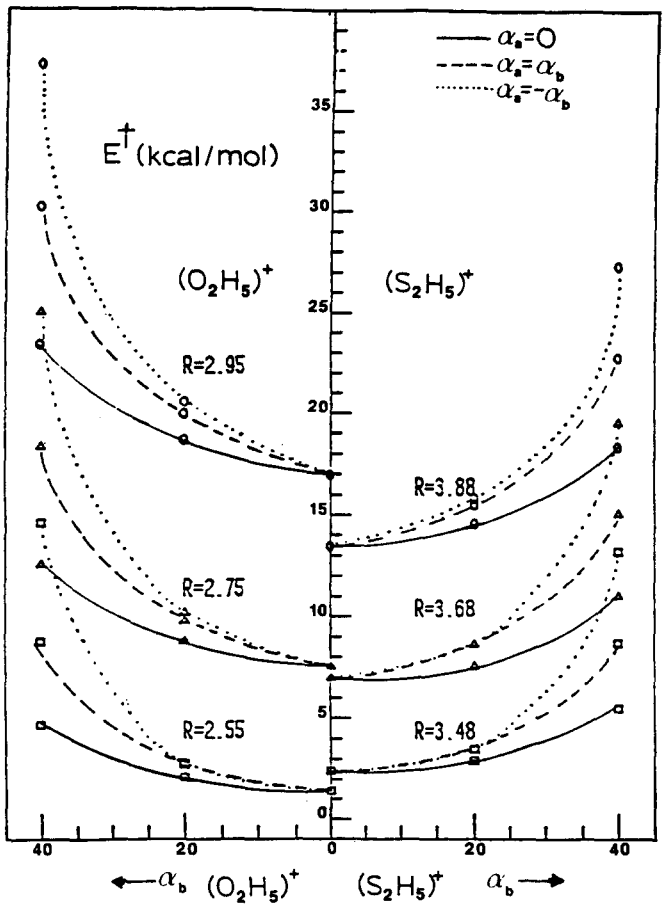

FIG. 5. Effects of angular distortions upon the proton transfer barrier $E\dagger$ (in kcal/mol).

the right side of the figure for $(S_2H_5)^+$ where it may be seen that the above trends hold for this system as well. In addition, the sensitivities of the oxygen and sulfur-containing systems to these angular distortions are quite similar to one another as indicated by the slopes of the curves. In all cases, 20° distortions produce only small barrier height increases while much more dramatic enlargements result from greater deformations. An important conclusion of this work is that the energetics of proton transfer in both systems are quite sensitive to angular deformations of the H-bond geometry as well as to stretches of the bond.

ACKNOWLEDGMENTS

We are grateful to Z. Latajka for sending a paper prior to publication. This research was funded in part by the National Institutes of Health (GM29391 and AM01059) and the Research Corporation. Computer time was made available by the SIU Computer Center.

[1] *Proton Transfer Reactions,* edited by E. Caldin and V. Gold (Chapman and Hall, New York, 1975); Faraday Discuss. Chem. Soc., No. 74 (1982); H. F. Koch, Acc. Chem. Res. **17,** 137 (1984).
[2] W. E. Farneth and J. I. Brauman, J. Am. Chem. Soc. **98,** 7891 (1976); J. M. Jasinski and J. I. Brauman, *ibid.* **102,** 2906 (1980); C. R. Moylan and J. I. Brauman, Annu. Rev. Phys. Chem. **34,** 187 (1983).
[3] M. Meot-Ner, J. Am. Chem. Soc. **106,** 278, 1257, 1265 (1984).
[4] F. M. Menger, Tetrahedron **39,** 1013 (1983); F. M. Menger, J. F. Chow, H. Kaiserman, and P. C. Vasquez, J. Am. Chem. Soc. **105,** 4996 (1983).
[5] R. Rossetti, R. Rayford, R. C. Haddon, and L. E. Brus, J. Am. Chem. Soc. **103,** 4303 (1981); R. R. Squires, V. M. Bierbaum, J. J. Grabowski, and C. H. DePuy, *ibid.* **105,** 5185 (1983).
[6] E. Grunwald, C. F. Jumper, and S. Meiboom, J. Am. Chem. Soc. **84,** 4664 (1962).
[7] S. L. Baughcum, Z. Smith, E. B. Wilson, and R. W. Duerst, J. Am. Chem. Soc. **106,** 2260 (1984); D. McMorrow, T. P. Dzugan, and T. J. Aartsma, Chem. Phys. Lett. **103,** 492 (1984).
[8] J. M. Clemens, R. M. Hochstrasser, and H. P. Trommsdorff, J. Chem. Phys. **80,** 1744 (1984).
[9] J. R. de la Vega, Acc. Chem. Res. **15,** 185 (1982); M. C. Flanigan and J. R. de la Vega, J. Chem. Phys. **61,** 1882 (1974); J. H. Busch and J. R. de la Vega, J. Am. Chem. Soc. **99,** 2397 (1977); J. H. Busch, E. M. Fluder, and J. R. de la Vega, *ibid.* **102,** 4000 (1980).
[10] B. O. Roos, W. P. Kraemer, and G. H. F. Diercksen, Theor. Chim. Acta **42,** 77 (1976); G. Karlström, B. Jönsson, B. Roos, and H. Wennerström, J. Am. Chem. Soc. **98,** 6851 (1976).
[11] W. Meyer, W. Jakubetz, and P. Schuster, Chem. Phys. Lett. **21,** 97 (1973).
[12] J.-J. Delpuech, G. Serratrice, A. Strich, and A. Veillard, Mol. Phys. **29,** 849 (1975).
[13] P. Merlet, S. D. Peyerimhoff, and R. J. Buenker, J. Am. Chem. Soc. **94,** 8301 (1972).
[14] P. A. Kollman and L. C. Allen, J. Am. Chem. Soc. **92,** 6101 (1970); C. A. Deakyne and L. C. Allen, *ibid.* **101,** 3951 (1979).
[15] M. D. Newton and S. Ehrenson, J. Am. Chem. Soc. **93,** 4971 (1971).
[16] J. Fritsch, G. Zundel, A. Hayd, and M. Maurer, Chem. Phys. Lett. **107,** 65 (1984).
[17] H. Tanaka and K. Nishimoto, J. Phys. Chem. **88,** 1052 (1984).
[18] J. Angyan and G. Naray-Szabo, Theor. Chim. Acta **64,** 27 (1983).
[19] H. Z. Cao, M. Allavena, O. Tapia, and E. M. Evleth, Chem. Phys. Lett. **96,** 458 (1983); S. Nagaoka, N. Hirota, T. Matsushita, and K. Nishimoto, *ibid.* **92,** 498 (1982).
[20] S. Ikuta, S. Hashimoto, and M. Imamura, Chem. Phys. **42,** 269 (1979).
[21] E. Clementi, J. Chem. Phys. **46,** 3851 (1967).
[22] Z. Latajka, S. Sakai, K. Morokuma, and H. Ratajczak, Chem. Phys. Lett. (submitted).
[23] B. T. Thole and P. T. van Duijnen, Biophys. Chem. **18,** 53 (1983).
[24] K. Pecul and R. Janoschek, Theor. Chim. Acta **36,** 25 (1974); K. Pecul, *ibid.* **44,** 77 (1983).
[25] S. Scheiner, J. Am. Chem. Soc. **103,** 315 (1981); Ann. N.Y. Acad. Sci. **367,** 493 (1981).
[26] R. Ditchfield, W. J. Hehre, and J. A. Pople, J. Chem. Phys. **54,** 724 (1971).
[27] P. J. Desmeules and L. C. Allen, J. Chem. Phys. **79,** 4731 (1980).
[28] S. Scheiner, J. Phys. Chem. **86,** 376 (1982); J. Chem. Phys. **77,** 4039 (1982).
[29] E. A. Hillenbrand and S. Scheiner, J. Am. Chem. Soc. **106,** 6266 (1984).
[30] W. J. Hehre, W. A. Lathan, R. Ditchfield, M. D. Newton, and J. A. Pople, QCPE **11,** 236 (1973).
[31] J. S. Binkley, R. A. Whiteside, R. Krishnan, R. Seeger, D. J. DeFrees, H. B. Schlegel, S. Topiol, L. R. Kahn, and J. A. Pople, QCPE, GAUSSIAN 80, Program No. 406 (1981).
[32] S. Scheiner, J. Chem. Phys. **80,** 1982 (1984).
[33] M. Meot-Ner and F. H. Field, J. Am. Chem. Soc. **99,** 998 (1977); K. Hiraoka and P. Kebarle, Can. J. Chem. **55,** 24 (1977).
[34] P. W. Atkins, *Physical Chemistry* (W. H. Freeman, San Francisco, 1982), p. 751.
[35] S. Scheiner and L. B. Harding, J. Am. Chem. Soc. **103,** 2169 (1981); J. Phys. Chem. **87,** 1145 (1983).
[36] M. M. Szczesniak and S. Scheiner, J. Phys. Chem. **77,** 4586 (1982); S. Scheiner, M. M. Szczesniak, and L. D. Bigham, Int. J. Quantum Chem. **23,** 739 (1983).
[37] J. B. Collins, P. v. R. Schleyer, J. S. Binkley, and J. A. Pople, J. Chem. Phys. **64,** 5142 (1976).
[38] T. H. Dunning, Jr. and P. J. Hay, in *Methods of Electronic Structure Theory,* edited by H. F. Schaefer (Plenum, New York, 1977), pp. 1–27; R. C. Raffenetti, J. Chem. Phys. **58,** 4452 (1973).
[39] J. S. Binkley and J. A. Pople, Int. J. Quantum Chem. **9,** 229 (1975); J. A. Pople, J. S. Binkley, and R. Seeger, *ibid.* **10,** 1 (1976).
[40] The remainder of the geometries, exclusive of $r(S^aH^c)$, were taken as the 4-31G structure in the first column of Table I.
[41] S. Scheiner, J. Chem. Phys. **75,** 5791 (1981).